

**${}^6\text{Li}(\alpha, d){}^8\text{Be}$  reaction and the importance of exchange processes\***M. B. Greenfield,<sup>†</sup> M. F. Werby,<sup>‡</sup> and R. J. Philpott*Department of Physics, Florida State University, Tallahassee, Florida 32306*

(Received 14 January 1974)

The  ${}^6\text{Li}(\alpha, d){}^8\text{Be}_{g.s.}$  reaction is studied in the expectation that exchange contributions will be enhanced relative to the more usual light particle stripping process. Angular distributions of deuterons were measured at bombarding energies of 20 and 24 MeV and are found to exhibit back-angle peaking characteristic of the exchange process. Calculations including only a direct stripping mechanism are not able to account for the back-angle peaking and disagree with the back-angle data by more than two orders of magnitude. A two-mode finite-range distorted-wave Born-approximation analysis including cluster exchange contributions accurately describes the observed backward peaking at both energies. The importance of exchange contributions is attributed to favorable kinematic conditions and large cluster amplitudes associated with the exchange process.

NUCLEAR REACTIONS  ${}^6\text{Li}(\alpha, d)$ ,  $E=20, 24$  MeV; measured  $\sigma(\theta)$ ,  $\theta=15^\circ-175^\circ$ . Enriched target. Two-mode, finite range DWBA analysis.  ${}^8\text{Be}$ ; calculated  $\alpha\oplus\alpha$  radial function.

## I. INTRODUCTION

Nuclear mass transfer reactions at energies where compound effects are expected to be minimal are generally treated as direct pickup or stripping processes. A light particle is either stripped from or transferred to the projectile which then carries away the majority of the forward momentum. Such reactions are characterized by forward peaked angular distributions. Many observed angular distributions are in accord with this description and attest to the frequent dominance of the direct stripping or pickup mechanism.

A complete theoretical treatment of any reaction requires antisymmetrization of the total wave function which gives rise, in general, to a variety of exchange terms in the transition amplitude. The most important<sup>1</sup> of these terms describes the situation which occurs when the incoming particle picks up from the target nucleus all but the particle or cluster to be detected and retains the majority of the forward momentum. As a result, the exchange amplitude generally yields a backward peaked contribution to the angular distribution. If this exchange effect is to be significant there must be a large cluster spectroscopic amplitude for the detected particle in the target nucleus as well as a high probability for the final state of the residual nucleus to be formed from the projectile plus the transferred core.

The  ${}^6\text{Li}(\alpha, d){}^8\text{Be}$  reaction was studied in the expectation that it would be a good example of an exchange dominated reaction. The direct contribution to the transition amplitude is inhibited by a

number of factors. The wave functions that describe the  $\alpha$  and  ${}^8\text{Be}$  systems as  $d\oplus d$  and  $d\oplus {}^6\text{Li}$  clusters,<sup>2</sup> respectively, are rather constricted in space due to the large separation energies of the respective fragments. The overlaps of the relative wave functions with the distorted waves are therefore confined to a small spatial region near the origin. For low partial waves, the distorted wave function is attenuated by absorption, while high partial waves are excluded by the angular momentum barrier. The cluster probabilities which weight the transition amplitudes are expected to be small, thus further reducing the light particle stripping contributions. On the other hand, the wave functions which describe the  ${}^6\text{Li}$  and  ${}^8\text{Be}$  systems as  $\alpha\oplus d$  and  $\alpha\oplus\alpha$  clusters, respectively, have relatively large amplitudes and are not tightly bound, suggesting that exchange contributions will be very important.

Data for this work were taken at two energies for consistency and far enough back in angle to reveal the shape of the last maximum. The expected enhanced back angle cross sections were observed and the angular distributions were reasonably well described by the calculations presented below. The  ${}^6\text{Li}(\alpha, d)$  reaction has already been investigated by other authors,<sup>3-5</sup> but the data were either too low in energy or lacked sufficient angular range for our purposes.

## II. EXPERIMENTAL METHOD

Angular distributions of deuterons from the  ${}^6\text{Li}(\alpha, d){}^8\text{Be}_{g.s.}$  reaction were measured at  $\alpha$  laboratory energies of 20 and 24 MeV. The beam was produced by the Florida State University super

FN tandem accelerator with intensities of 100–300 nA on target. Targets of 99.8% isotopically enriched  ${}^6\text{Li}$  were prepared by evaporation of the enriched metal onto thin plastic backings. The targets were stored and transported under vacuum of  $10^{-4}$  Torr to prevent contamination. Target thickness was continuously monitored by observing elastically scattered  $\alpha$  particles with a fixed geometry counter. Neither deterioration of the target nor target nonuniformity produced any appreciable error, since the deuteron yield was normalized to the  $\alpha$  elastic yield from the fixed geometry counter.

Deuterons were measured with particle telescopes. The thickness of the surface-barrier transmission counters varied from 40–400  $\mu\text{m}$  depending on the deuteron energy observed (typically ranging from about 4 to 20 MeV). Care was taken so that the deuteron consistently lost some 20–50% of its energy in the transmission counter, thus providing satisfactory particle identification of deuterons. Figure 1 shows a typical particle identification spectrum containing proton and deuteron groups. Heavier particles were not observed since they were generally stopped in the transmission counter. Figure 2 shows a typical energy spectrum of particles gated by the deuteron peak in the particle identification spectrum. The sharp peak corresponds to the  ${}^8\text{Be}_{g.s.}$ , the broad peak corresponds to the first excited state of  ${}^8\text{Be}$  which has a width of 1.5 MeV<sup>6</sup> and contains additional continuum contributions resulting from the break-up of  ${}^6\text{Li}$ . The identification and separation of the  ${}^8\text{Be}_{g.s.}$  peak is such that there is little error due to

background subtraction from peak areas.

The relative error in the data, presented in Sec. IV, is due primarily to counting statistics and is typically smaller than the size of the data points. The absolute normalization of the data was determined by measuring 6.86 MeV proton elastic scattering at  $95^\circ$  and comparing with previously measured absolute cross sections.<sup>7</sup> Error in the absolute normalization of the data is due to error in determination of deuteron solid angles, error in beam current normalization, counting statistics and the absolute error in the proton elastic scattering data mentioned above. The total uncertainty in the absolute normalization of the data is  $\pm 9\%$ .

### III. THEORY

The data obtained in this work were analyzed within an exact finite-range two-mode multi-interaction distorted wave Born approximation (DWBA) formalism which has been fully described elsewhere.<sup>8</sup> We mention here only the specific details essential to the understanding of the ensuing analysis:

The direct stripping process is represented as

$$(\alpha = d \oplus d) + {}^6\text{Li} \rightarrow ({}^8\text{Be} = d \oplus {}^6\text{Li}) + d, \quad (1)$$

where the deuteron is stripped from the projectile into the target, forming  ${}^8\text{Be}_{g.s.}$  as the residual nucleus. The DWBA transition amplitude for the direct process is

$$T^D = \langle f | V_{dd} + V_d {}^6\text{Li} - U_d {}^8\text{Be} | i \rangle, \quad (2)$$

where  $V_{xy}$  designates the interaction between clus-

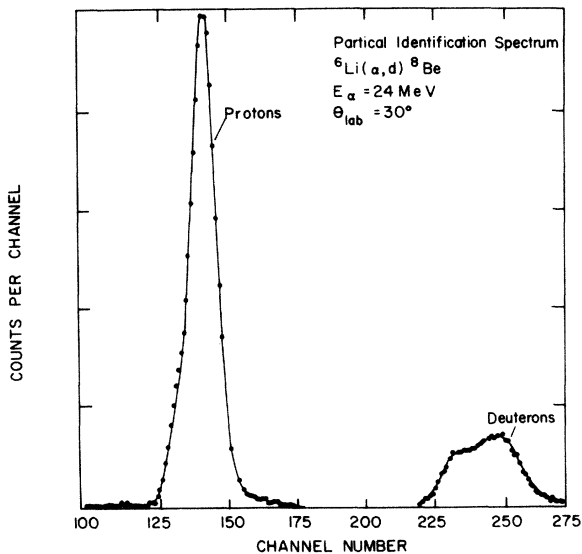


FIG. 1. Particle identification spectrum from bombardment of  ${}^6\text{Li}$  with 24 MeV  $\alpha$  particles.

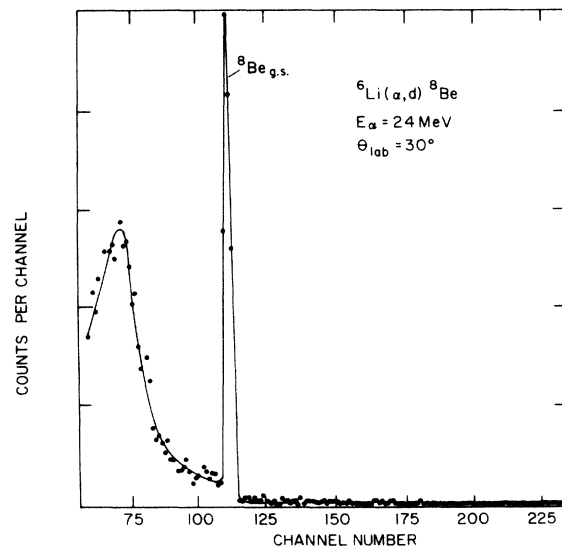


FIG. 2. Energy spectrum of events gated as deuterons from the  ${}^6\text{Li}(\alpha, d){}^8\text{Be}$  reaction at 24 MeV.

TABLE I. Interaction potentials.

System	$V_0$ (MeV)	$R_0$ (fm)	$a_0$ (fm)
$d+d$ (1s)	66	2	0.8
${}^6\text{Li}+d$ (1d)	91.3	2.6	0.7

ters  $x$  and  $y$ . Although it is common to assume that the contribution of  $V_{d\text{Li}}$  cancels with that of the exit channel optical model potential  $U_{d\text{Be}}$ , this approximation was not considered appropriate here. All three terms were therefore included in the present analysis. The exchange process is represented as

$$\alpha + ({}^6\text{Li} = \alpha' \oplus d) \rightarrow ({}^8\text{Be} = \alpha' \oplus \alpha) + d, \quad (3)$$

where an  $\alpha$  particle is picked up from the target and combines with the projectile to form  ${}^8\text{Be}_{g.s.}$ . The transition amplitude for the exchange process is

$$T^E = \langle f | V_{d\alpha} + V_{d\alpha'} - U_{d\text{Be}} | i \rangle. \quad (4)$$

Note that one of the  $\alpha$ 's is primed to indicate that it originates in the target nucleus. Although two of the interactions have the same functional form, the corresponding two matrix elements are different because the interactions are functions of different coordinates. Following the terminology introduced previously,<sup>8</sup>  $V_{dd}$  and  $V_{d\text{Li}}$  give rise to light particle stripping and heavy particle knock-out, respectively, while  $V_{d\alpha'}$  and  $V_{d\alpha}$  give rise to heavy particle stripping and light particle knock-out.

The terms  $|i\rangle$  and  $\langle f|$  contain both bound state and distorted wave information appropriate for the particular transfer process. In particular, each interaction  $V$  between bound state clusters  $x\oplus y$  and  $y\oplus z$  in the scattering amplitude represents a six dimensional integral of the form

$$T^V = \int \psi_f \phi_{yz} V \phi_{xy} \psi_i d\tau,$$

where the  $\psi$ 's and  $\phi$ 's designate continuum and bound state wave functions, respectively. In the present analysis, these integrals are evaluated exactly, as described in Ref. 8. A possible spin-orbit coupling in the exit channel is ignored. While

TABLE II. Optical model parameters.

System	$V_0$ (MeV)	$R_0$ (fm)	$a_0$ (fm)	$W_V$ (MeV)	$R_I$ (fm)	$a_I$ (fm)
${}^6\text{Li}+\alpha$	194	3.0	0.6	15	3.5	0.5
${}^8\text{Be}+d$	63.1	2.75	0.991	10	2.75	0.991

the computer code FANLU2 automatically includes interference terms between the direct and exchange contributions wherever necessary, these terms were identically zero in the present calculations by virtue of the angular momentum selection rules.<sup>8</sup>

#### IV. CHOICE OF INTERACTION PARAMETERS

The initial and final states which appear in the above expressions for the transition amplitudes contain optical model wave functions representing the elastic scattering process in the initial and final channels, respectively, and form factors which reflect the cluster structure of the involved nuclei. The model parameters which determine these functions were fixed in order to avoid the prohibitive tedium and ambiguity of an extended parameter search. In the present instance, we have used optical model parameters that were used to describe the  ${}^6\text{Li}+\alpha$  channel of the  ${}^7\text{Li}-({}^3\text{He}, \alpha){}^6\text{Li}$  reaction as well as elastic scattering data on other  $1p$  shell nuclei.<sup>9</sup>

The  ${}^6\text{Li}+d$  and the  $d+d$  bound relative wave functions were determined by varying the strength of Woods-Saxon wells of standard geometry until the observed binding energies were reproduced.<sup>10</sup> The geometries and corresponding depths are given in Table I. The  $\alpha+d$  relative wave function was determined<sup>11</sup> by folding an  $\alpha$ -nucleon potential given by Sack, Biedenharn, and Breit<sup>12</sup> with the deuteron relative wave function  $\phi_d(r)$  to produce an effective  $\alpha+d$  potential of form

$$V_{\alpha d}(\rho) = \int \phi_d(r) [V_n(\vec{\rho} + \frac{1}{2}\vec{r}) + V_p(\vec{\rho} - \frac{1}{2}\vec{r})] \phi_d(r) dr. \quad (5)$$

This potential was then employed to generate a  $2s$  or  $1d$   $\alpha+d$  relative wave function, as described in Ref. 11. For the  $2s$  function, a reduction of less than 5% in the strength of the potential was required to reproduce the observed binding energy of the  $\alpha+d$  system. For the  $1d$  state the strength was increased by approximately the same amount in order to reproduce the observed cluster separation energy.

A suitable potential model for the  ${}^8\text{Be}+d$  channel is more difficult to obtain because the instability of the  ${}^8\text{Be}$  nucleus prevents direct observation of elastic scattering. At the same time, the loose structure of the  ${}^8\text{Be}$  nucleus suggests that appropriate potential parameters may be different from those associated with standard targets. In this work, the real part of the  ${}^8\text{Be}+d$  potential was generated by folding the  $\alpha+d$  potential derived above with the unbound  ${}^8\text{Be} \alpha+\alpha$  relative wave function described below. The resulting numerical potential could be well represented by a

Woods-Saxon form. The imaginary part of the  ${}^8\text{Be} \oplus d$  potential was arbitrarily assumed to have the same radial form as the real part and a depth of 10 MeV. The parameters of the equivalent Woods-Saxon potential are listed in Table II.

In addition to the above potentials and wave functions, one needs, finally, a model for the relative wave function describing the  $\alpha \oplus \alpha$  cluster structure in  ${}^8\text{Be}$ . The continuum nature of this wave function, which arises because the  ${}^8\text{Be}$  ground state lies above the threshold for  $\alpha$  emission, introduces certain well known<sup>13</sup> formal complications into the treatment of the distorted wave overlaps. In the present instance these complications are minimized by the strong influence of the Coulomb barrier, which effectively decouples the  ${}^8\text{Be}$  interior from the asymptotic region. At the observed<sup>14</sup> resonance energy of 95 keV, the outer classical turning point is not reached until the two  $\alpha$  particles are 60 fm apart. Within this radius, the  ${}^8\text{Be}$  wave function behaves like a bound state and has been treated as such in the calculations described here. Our  ${}^8\text{Be}$  wave functions are matched to the correct asymptotic form at 60 fm, but normalized to unity over the region  $0 \leq r \leq 60$  fm. At 60 fm, the magnitude of the radial function  $R(r)$  has fallen to some  $3 \times 10^{-4}$  times the magnitude at 3.5 fm and the radial integrals required to calculate the exchange transition amplitudes appear to have converged.

The nodeless  ${}^8\text{Be}$  wave function shown in Fig. 3 was generated from the  $\alpha$ - $\alpha$  potential of Ali and Bodmer<sup>15</sup> by adjusting the strength slightly (about 4 parts in 1000) to bring the  $s$  wave into resonance at 95 keV. The  $s$ -wave Ali-Bodmer potential has the form

$$V(r) = V_R \exp(-\mu_R^2 r^2) - V_A \exp(-\mu_A^2 r^2) + 4e^2/r, \quad (6)$$

where  $V_A = 130$  MeV and  $\mu_A = 0.475$  fm<sup>-1</sup> are the strength and inverse range of an attractive compo-

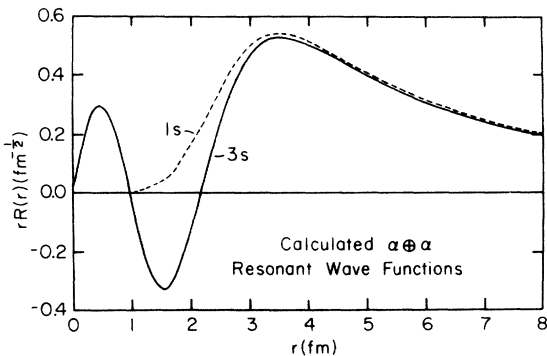


FIG. 3. Calculated resonant wave functions for the  $\alpha \oplus \alpha$  representation of the  ${}^8\text{Be}$  ground state.

nent which was fitted to  $g$ -wave phase shifts obtained from  $\alpha$ - $\alpha$  scattering experiments, and  $V_R = 500$  MeV,  $\mu_R = 0.7$  fm<sup>-1</sup> are the strength and inverse range of an additional short range repulsive component. The last term in Eq. (6) represents the Coulomb interaction.

The repulsive part of the nuclear interaction prevents the formation of bound states in the potential, with the result that the calculated resonance wave function has a  $1s$  character. The lack of nodes in this wave function is inconsistent with results<sup>16</sup> obtained from the more realistic cluster model, in which the wave function for  ${}^8\text{Be}$  is represented by two interacting  $\alpha$  particles and the antisymmetry with respect to nucleon coordinates is properly taken into account. The cluster model wave function has a  $3s$  character and exhibits two interior nodes. A  $3s$  wave function may be obtained from the potential of Ali and Bodmer if the repulsive nuclear part is omitted. The resulting wave function is also shown in Fig. 3. Somewhat surprisingly, perhaps, the modified potential reproduces the measured  $s$ -wave phase shifts at least as well as the Ali-Bodmer potential over the same range of energies  $0 \leq E_{COM} \leq 12$  MeV, to which the Ali-Bodmer potential was originally fitted. There is thus no compelling reason to prefer the calculated  $1s$  function over the  $3s$  function. A more realistic  $\alpha$ - $\alpha$  interaction would be expected to exhibit strong nonlocality at short ranges which would tend to damp<sup>17</sup> the inner oscillations of the wave function relative to the  $3s$  wave function of the local potential well (Perey effect). One might therefore expect that a better relative motion wave function would lie between the two extremes calculated above. This expectation appears to be borne out by explicit cluster model calculations.<sup>16</sup> In the

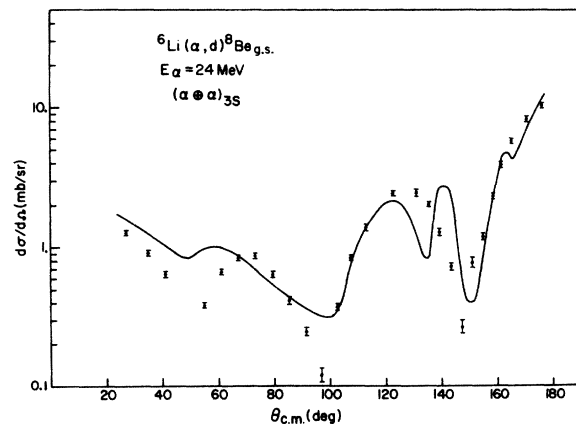


FIG. 4. A comparison of the 24 MeV experimental angular distribution from the  ${}^6\text{Li}(\alpha, d){}^8\text{Be}$  reaction with the calculated cross section, assuming an  $(\alpha \oplus \alpha)_{3s}$  resonant final state wave function.

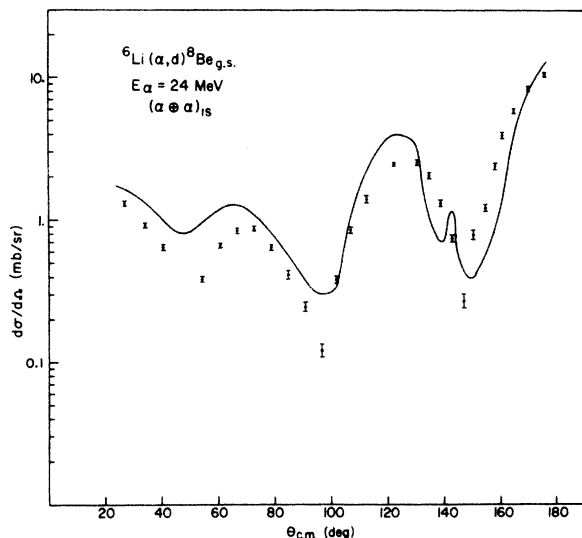


FIG. 5. A comparison of the 24 MeV experimental angular distribution from the  ${}^6\text{Li}(\alpha, d){}^8\text{Be}$  reaction with the calculated cross section, assuming an  $(\alpha \otimes \alpha)_{1s}$  resonant final state wave function.

following work, both form factors of Fig. 3 have been used in an attempt to bracket the uncertainties introduced via the  ${}^8\text{Be}$  resonant wave function.

When the potentials and form factors have been fixed, the only variable parameters entering into the calculation of the transition amplitudes are products of spectroscopic amplitudes.<sup>8</sup> Although these amplitudes may be considered adjustable to some extent, their permissible range of variation is strongly limited in practice by contemporary cluster-model expectation.

## V. RESULTS

The measured deuteron angular distributions from the  ${}^6\text{Li}(\alpha, d){}^8\text{Be}$  reaction at 24 MeV is shown in Figs. 4 through 6 and at 20 MeV in Fig. 7. As mentioned earlier, the relative errors are represented by the size of the bar on each data point and the total absolute error is about  $\pm 10\%$ .

The curves represent calculations performed by the two-mode multi-interaction exact finite-range code FANLU2 which takes into account all reaction processes discussed in the theory section. As mentioned previously, the optical parameters and interaction potentials were fixed in advance and only the products of spectroscopic amplitudes were allowed to vary. The present calculations include only the  $1d$  component of the  ${}^6\text{Li} \oplus d$  relative wave function and the  $2s$  component of the  $\alpha \oplus d$  relative wave function. Values of 0.013 for the product  $S_{d\text{Be}}^{\alpha} S_{\alpha d}^{\alpha}$  and 3.25 for the product  $S_{\alpha\alpha}^{\text{Be}} S_{\alpha d}^{\text{Li}}$  were employed to generate the curves shown in Figs. 4 through 7.  $S_{xy}^z$  is the spectroscopic factor for the

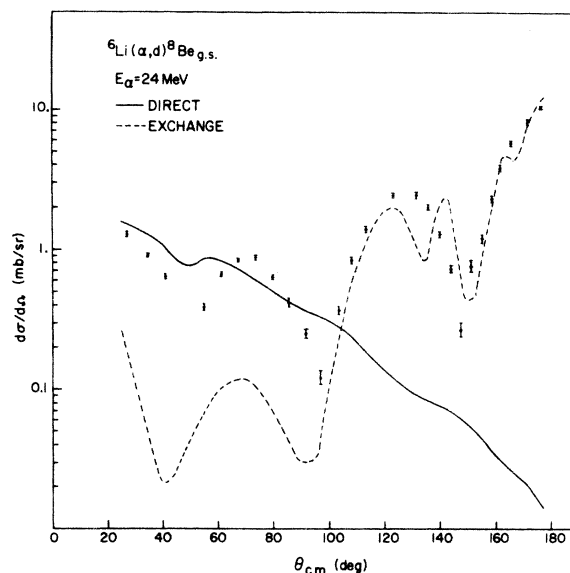


FIG. 6. A comparison of the 24 MeV experimental angular distribution from the  ${}^6\text{Li}(\alpha, d){}^8\text{Be}$  reaction with the direct and exchange contributions to the cross section.

breakup of  $z$  into  $x \oplus y$ . These values were obtained by best  $\chi^2$  fits to the data.

Figure 4 shows the calculated 24 MeV cross section which results when the  $3s$   ${}^8\text{Be}$  resonant wave function is used and Fig. 5 shows the corresponding cross section obtained from the  $1s$   ${}^8\text{Be}$  resonant motion wave function. Both calculations provide reasonable fits to the data. The separate contributions of the direct and exchange terms to the calculated angular distribution at 24 MeV are shown in Fig. 6, to illustrate their relative importance. The direct part taken alone falls below the data by over 2.5 orders of magnitude at back angles. The exchange contribution roughly repro-

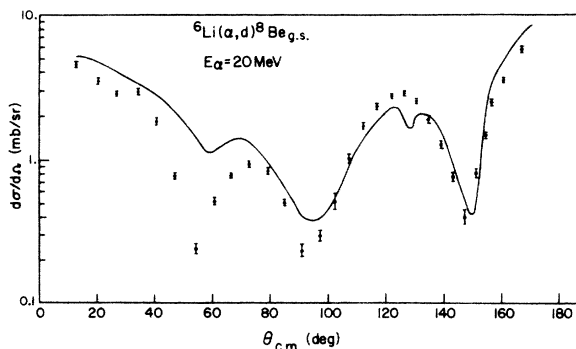


FIG. 7. A comparison of the 20 MeV angular distribution from the  ${}^6\text{Li}(\alpha, d){}^8\text{Be}$  reaction with the calculated cross section.

duces the back angle data and, when combined with the direct contribution, provides a reasonably good fit over the entire angular range of the data. The 20 MeV data is also reasonably well reproduced when the exchange contribution is included, as illustrated in Fig. 7.

Some pilot calculations were carried out to investigate effects associated with form factor components not included in the calculations reported above. The  ${}^6\text{Li}\oplus d$  relative wave function is expected to contain a  $2s$  component in addition to the  $1d$  component. The  $2s$  component provides a small additional contribution to the cross section which is strongly peaked in the forward direction. However, a significant contribution to the cross section is only obtained if an inordinately large product of spectroscopic factors is assumed. It is therefore quite permissible to omit this component of the  ${}^6\text{Li}\oplus d$  wave function.

Similarly, the  $\alpha\oplus d$  relative wave function is expected to contain a  $1d$  admixture with a probability of 2–4%.<sup>11</sup> The contribution of this component to the calculated cross section may somewhat alter the normalization of the exchange term, but is not expected to exert a strong influence on the shape. Preliminary calculations which include the  $1d$  contribution tend to support this expectation. A fairly smooth cross section is obtained which peaks at backward angles. Although the  $1d$  contribution has an appreciable influence on the magnitude of the spectroscopic factors extracted by fitting the observed back-angle cross section, it was not possible to improve the description of the various minima in the observed cross section by including this contribution. Further examination of this contribution was prevented by the prohibitive time required for such calculations.

The product of spectroscopic factors which governs the strength of the exchange contribution contains a spectroscopic factor for the breakup of  ${}^8\text{Be}$  into two  $\alpha$  particles. It is reasonable to assume that the magnitude of this spectroscopic factor is approximately 2, close to the maximum value associated with a pure  $\alpha\oplus\alpha$  configuration (a factor of 2 in the spectroscopic factor arises from the symmetry with respect to  $\alpha$ -cluster exchange of the fully antisymmetrized  ${}^8\text{Be}$  wave function, see Appendix). The present value of 3.25 for the product of spectroscopic factors therefore appears to be about twice as large as one might reasonably expect. A rough calculation including between 2 and 4% of the  $1d$  term of the  $\alpha\oplus d$  cluster reduces the product of spectroscopic factors from 3.25 to less than 2.00. The rather strong contribution of the  $1d$  component arises because the angular momentum matching condition favors the transfer of two units of angular momentum.

## VI. CONCLUSION

Angular distributions of the  ${}^6\text{Li}(\alpha, d){}^8\text{Be}$  reaction were measured at 20 and 24 MeV in order to investigate the importance of exchange processes. The large differential cross section observed at backward angles is typical of a strong exchange process which, on the basis of cluster considerations, is expected to dominate the reaction. An analysis of the angular distributions including both direct and exchange amplitudes is in good agreement with the data.

## ACKNOWLEDGMENTS

The authors would like to thank G. Vourvopoulos, G. Gunn, G. Morgan, and W. J. Courtney for helping with the data taking and are very grateful to S. Edwards and K. Kemper for a critical review of the manuscript.

## APPENDIX: SUM RULE ARGUMENT FOR $S=2$

Assume that the  ${}^8\text{Be}$  internal wave function has a structure describable as two nonoverlapping  $\alpha$  particles in a relative bound state, viz

$$\psi_{\text{Be}}(1234, 1'2'3'4') = N\mathcal{G}\psi_{\alpha\alpha}(121'2'; 343'4')$$

where

$$\psi_{\alpha\alpha}(121'2'; 343'4') \equiv \chi(\vec{r})\chi_{\alpha}(121'2')\chi_{\alpha}(343'4').$$

Unprimed coordinates refer to protons, primed coordinates to neutrons,  $N$  is a normalization constant, and  $\mathcal{G}$  is an appropriate antisymmetrization operator. The wave functions  $\chi_{\alpha}$  are assumed to be normalized and antisymmetrized. They depend only on the internal coordinates (spin and relative spatial coordinates) appropriate to the nucleon coordinates given as arguments.

The relative function  $\chi(\vec{r})$  may be written as a superposition of even and odd functions with respect to the parity operation  $\vec{r} \rightarrow -\vec{r}$ . When  $\psi_{\alpha\alpha}$  is totally antisymmetrized, contributions from the odd component of  $\chi(\vec{r})$  are automatically removed. There is therefore no loss of generality if  $\chi(\vec{r})$  is assumed at the outset to be an even function of  $\vec{r}$ . [This condition is of course assured if  $\chi(\vec{r})$  is an angular momentum eigenfunction with even  $L$ .]

The antisymmetrizer  $\mathcal{G}$  contains  $(4!/2!2!)^2 = 36$  distinct partitions. The normalization constant can be obtained from the result

$$\begin{aligned} \langle \psi_{\text{Be}} | \psi_{\text{Be}} \rangle &= 1 \\ &= N^2 \langle \psi_{\alpha\alpha} | \mathcal{G}^2 | \psi_{\alpha\alpha} \rangle \\ &= 36N^2 \langle \psi_{\alpha\alpha} | \mathcal{G} | \psi_{\alpha\alpha} \rangle. \end{aligned}$$

The last matrix element reduces to 2, since there are two partitions of the coordinates, namely (121'2'; 343'4') and (343'4'; 121'2') which each provide unit overlap. Thus we obtain  $N^2 = 1/72$ .

The spectroscopic factor can now be calculated for the state  $\psi_{\alpha\alpha}$  which exhausts the sum rule.

It is

$$S = (4! / 2! 2!)^2 |\langle \psi_{\alpha\alpha} | \psi_{Be} \rangle|^2 = 36N^2 |\langle \psi_{\alpha\alpha} | \alpha | \psi_{\alpha\alpha} \rangle|^2.$$

The factor of 2 is seen to arise from the symmetry with respect to  $\alpha$ -cluster exchange of the fully antisymmetrized  ${}^8\text{Be}$  wave function.

\*Work supported in part by the National Science Foundation Grants Nos. NSF-GU-2612, NSF-GP-15855, and NSF-GJ-367.

<sup>†</sup>Present address: Department of Physics, Florida A&M University, Tallahassee, Florida 32307.

<sup>‡</sup>Present address: Department of Physics, Case Western Reserve University, Cleveland, Ohio 44106.

<sup>1</sup>L. Madansky and G. E. Owen, Phys. Rev. 99, 1608 (1955).

<sup>2</sup>K. Wildermuth and W. McClure, *Cluster Representations of Nuclei* (Springer, Berlin, 1966).

<sup>3</sup>B. Feidman and J. L. Yntema, Nucl. Phys. 12, 298 (1959).

<sup>4</sup>H. E. Wegner, W. S. Hall, and D. W. Miller, in *Direct Interactions and Nuclear Reaction Mechanisms*, edited by E. Clementel and C. Villi (Gordon and Breach, New York, 1963), p. 1004.

<sup>5</sup>J. Cerny, B. G. Harvey, and R. H. Pehl, Nucl. Phys. 29, 120 (1961).

<sup>6</sup>T. Lauritsen and F. Ajzenberg-Selove, Nucl. Phys. 78, 1 (1966).

<sup>7</sup>H. G. Bingham, A. R. Zander, K. W. Kemper, and N. R. Fletcher, Nucl. Phys. A173, 265 (1971).

<sup>8</sup>S. Edwards, D. Robson, T. L. Talley, W. J. Thompson,

and M. F. Werby, Phys. Rev. C 8, 456 (1973).

<sup>9</sup>M. F. Werby and S. Edwards, Bull. Am. Phys. Soc. 18, 626 (1973); Nucl. Phys. (to be published); and T. Gray, T. Fortune, W. Trost, and N. Fletcher, *ibid.* A144, 129 (1970).

<sup>10</sup>N. Austern, Phys. Rev. 136, B1743 (1964).

<sup>11</sup>M. F. Werby, M. B. Greenfield, K. W. Kemper, D. L. McShan, and S. Edwards, Phys. Rev. C 8, 106 (1973).

<sup>12</sup>S. Sack, L. C. Biedenharn, and G. Breit, Phys. Rev. 93, 321 (1954).

<sup>13</sup>R. Huby and J. R. Mines, Rev. Mod. Phys. 37, 406 (1965); C. M. Vincent and H. T. Fortune, Phys. Rev. C 2, 782 (1970).

<sup>14</sup>T. Lauritsen and F. Ajzenberg-Selove, Nucl. Phys. 78, 1 (1966).

<sup>15</sup>S. Ali and A. R. Bodmer, Nucl. Phys. 80, 99 (1966); S. A. Afzal, A. A. X. Ahmad, and S. Ali, Rev. Mod. Phys. 41, 247 (1969).

<sup>16</sup>S. Okai and S. C. Park, Phys. Rev. 145, 787 (1966).

<sup>17</sup>F. G. Perey, in *Direct Interactions and Nuclear Reaction Mechanisms*, edited by E. Clementel and C. Villi (see Ref. 4); N. Austern, Phys. Rev. 137, B752 (1965); J. F. Reading, *ibid.* 153, 1377 (1967).